

***In vitro* bioaccessibility of fish oil-loaded hollow solid lipid
micro- and nanoparticles**

Journal:	<i>Food & Function</i>
Manuscript ID	FO-ART-06-2020-001591.R1
Article Type:	Paper
Date Submitted by the Author:	28-Aug-2020
Complete List of Authors:	Yang, Junsu; University of Nebraska-Lincoln, Department of Food Science and Technology Ciftci, Ozan Nazim; University of Nebraska-Lincoln, Department of Food Science and Technology

***In vitro* bioaccessibility of fish oil-loaded hollow solid lipid micro- and nanoparticles**

Junsi Yang and Ozan N. Ciftci*

Department of Food Science and Technology, University of Nebraska-Lincoln, Lincoln, NE

68588-6205, USA

*Corresponding author

E-mail: ciftci@unl.edu

Tel: +1-402-4725686

Abstract

Fish oil-loaded hollow solid lipid micro- and nanoparticles were prepared by atomization of the CO₂-expanded lipid mixture. The obtained particles were spherical and free-flowing with an average particle size of 6.9 µm. Fish oil loading efficiency was achieved at 92.3% (w/w). The *in-vitro* digestive stability, lipid digestibility and EPA and DHA bioaccessibility of the fish oil-loaded particles were examined using an *in-vitro* sequential digestion model. The mean particle diameter increased markedly after oral (15.2 µm) and gastric (32.4 µm) digestion and then decreased after the small intestinal stage (24.0 µm). Fish oil-loaded particles remained spherical and intact but mainly agglomerated on the top phase throughout the oral and gastric digestion. However, a mixed digesta was formed after the small intestinal digestion, which contained digested broken particle pieces, undigested fish oil-loaded particles, free fatty acids, monoacylglycerols and micelles. The extent of lipolysis was significantly increased for the 30% fish oil-loaded particles as compared to physical mixtures of empty hollow solid lipid particles or bulk FHSO and fish oil ($p < 0.05$). Moreover, EPA and DHA bioaccessibility was significantly improved from 9.7 to 18.2% with the 30% fish oil-loaded particles ($p < 0.05$).

Keywords: Fish oil; Encapsulation; *In-vitro* digestion; Lipid digestibility, Bioaccessibility

1. Introduction

In recent years, there is a growing interest in “clean” foods, as well as the demand for functional foods and beverages beyond basic nutritional needs. The food industry has made considerable efforts in developing food products containing functional bioactive components. Long-chain polyunsaturated fatty acids (PUFAs), especially eicosapentaenoic acid (EPA) and docosahexaenoic acid (DHA), have received much attention due to their associated health benefits. A diet rich in long-chain omega-3 fatty acids has the potential to reduce coronary heart disease, immune disorders, diabetes, some types of cancer, and depression.¹⁻³ In addition, DHA has an important role in neural and visual development in infants.^{4,5}

Fish oil abundant in long-chain PUFAs is one of the main sources of EPA and DHA. However, the incorporation of fish oil into foods is challenging due to its low solubility in aqueous food systems, and high vulnerability to oxidation.⁶⁻⁸ Encapsulation has been used as an effective method to develop dry powder formulations in order to stabilize long-chain omega-3 PUFAs and mask the inherent fishy taste and odor.^{9,10} Encapsulated omega-3 PUFAs have been used to produce a variety of fortified food products.^{9,11-13} Different matrices, such as β -cyclodextrin,¹⁴ gelatin,¹⁵ polysaccharide,¹⁶ protein,¹⁷⁻²¹ and starch^{22, 23} have also been investigated to encapsulate fish oil. In the above-mentioned approaches, after forming a homogenous emulsion, a drying step follows. In particular, spray drying has been widely used as the drying step to develop encapsulated fish oil in the powder form. Nevertheless, it exhibits disadvantages such as high temperature to cause PUFAs oxidation and degradation.

Recently, formation of fish oil-loaded hollow solid lipid micro- and nanoparticles using a single step process based on supercritical carbon dioxide (SC-CO₂) technology was reported by our group.^{6,24} Fish oil was loaded into hollow solid micro- and nanoparticles made of fully

hydrogenated soybean oil (FHSO). This was the first study loading fish oil into a solid fat in the dry free-flowing powder form. It was found that this new form of fish oil carrier is a promising approach to develop easy to use free-flowing powder fish oil formulation with improved oxidative stability. However, the performance of the fish oil-loaded hollow solid lipid particles to deliver fish oil during digestion is not known.

Stability and release behavior of fish oil carrier systems during gastrointestinal (GI) tract transit have attracted interest recently.^{16,18,20} Most of the reported studies focused on emulsion systems.^{16,25-26} It is important that PUFAs need to be released from food matrix post-ingestion and fully absorbed within the upper GI tract to exert their health benefits.²⁷ Typically, the ingested triacylglycerols go through hydrolysis by gastric and pancreatic lipases to activate the digestion of encapsulated oil, leading to free fatty acids and monoacylglycerols formation.^{28,29} Consequently, these lipid digestion products interact with small intestine secretions (bile salts and phospholipids) to form mixed micelles, which transport the free fatty acids and monoacylglycerols to the epithelium cells for absorption.^{21,30} Digestion and bioavailability of the encapsulated oil can be influenced by many factors, including particle size, nature and composition of the wall material, lipid type, other compounds consisting of the matrice, and digestion fluids.³¹⁻³⁴ In particular, there is evidence showing that EPA and DHA in triacylglycerols are structurally resistant to lipolysis, possibly due to the location of double bonds along the fatty acid chains and/or the positional distribution of these fatty acids within a triacylglycerol.³⁵ Therefore, strategies have been sought to improve EPA and DHA digestion and bioavailability, including those based on emulsification.³⁶ There are relatively few studies on *in-vitro* digestibility of micro- and nano-encapsulated fish oil in dry form, as well as the bioaccessibility of PUFAs after simulated digestion process. A study of *in-vitro* evaluation of spray-dried hydrocolloid-based encapsulated fish oil has been carried out to

understand its potential in controlled release delivery system.²⁰ The released oil after sequential digestion was <2% and 36% for caseinate and whey protein-based Maillard reaction product microcapsules, respectively. This finding suggests that the digestibility of the carrier is an important factor affecting bioavailability of the encapsulated oil. In another, *in-vitro* release of encapsulated tuna oil from whey protein isolate-gum Arabic complex coacervates was examined.³⁷ To the best of our knowledge, there is no report on the *in-vitro* evaluation of digestibility and bioaccessibility of the fish oil in solid lipids.

Therefore, the present study aimed to investigate the *in-vitro* digestive stability, digestibility, and EPA and DHA bioaccessibility of fish oil loaded in hollow solid lipid particles using a simulated digestion model.

2. Materials and methods

2.1. Materials

Fully hydrogenated soybean oil (FHSO) was kindly provided by ConAgra Brands Inc. (Omaha, NE, USA). Liquid CO₂ (99.99% purity) was purchased from Matheson (Lincoln, NE, USA). Fish oil (100% purity) from menhaden was obtained from Santa Cruz Biotechnology (Dallas, TX, USA).

α -Amylase from *Bacillus subtilis* was purchased from MP Biomedicals LLC (Solon, OH, USA). Pepsin from porcine gastric mucosa, pancreatin from porcine pancreas, lipase from porcine pancreas, and bile extract from porcine were all purchased from Sigma-Aldrich Co. (St. Louis, MO, USA). Lipase A “Amano” 12 lipase A12 (from fungus *Aspergillus niger*, 132000 U g⁻¹) was generously provided by Amano Enzyme Inc. (Elgin, IL, USA). All other chemicals, reagents, and

solvents were purchased from Fisher Scientific International, Inc (Fair Lawn, NJ, USA) and were of analytical or HPLC grade.

2.2. Production of the fish oil-loaded hollow solid lipid micro- and nanoparticles using SC-CO₂

Fish oil-loaded hollow solid lipid micro- and nanoparticles were produced using a home-made SC-CO₂ particle formation system. The details and the operating procedure of the particle formation system were previously reported.^{6,24} Briefly, after injecting predetermined amount of molten FHSO, fish oil was injected into the high-pressure expansion vessel to achieve an initial fish oil concentration of 30% (w/w). The particle formations were performed at the processing conditions of 200 bar expansion pressure, 50 μm nozzle diameter, and 57 °C expansion vessel temperature, which were optimized previously.²⁴ The liquid lipid mixture and the SC-CO₂ was mixed at 1000 rpm for 1 h to obtain a SC-CO₂-expanded lipid mixture. Then, the magnetic drive was stopped and waited for 10 min to stabilize the SC-CO₂-expanded lipid mixture. The pressure of the syringe pump was set at 210 bar, the CO₂ inlet valve was opened, and depressurization valve was subsequently opened. Consequently, the SC-CO₂-expanded lipid mixture was atomized through the nozzle. Upon atomization, solid lipid particles loaded with fish oil were formed due to natural cooling by Joule-Thomson effect. Production of empty hollow solid lipid particles (devoid of fish oil) was carried out as control.

2.3. Determination of fish oil loading efficiency

Fish oil-loaded solid lipid particles (~ 7 mg) was methylated according to Belayneh *et al.*³⁸ Briefly, 1.5 mL of 2.5% (v/v) sulfuric acid in methanol (containing 0.01% w/v butylated hydroxyl toluene, BHT), 400 μL of toluene, and 200 μL of a triheptadecanoin solution (10 mg/mL in toluene) were added into each tube. The tubes were capped under flushed nitrogen and heated at 90 °C for

1.5 h. Upon cooling, 1 mL of distilled water and 1.5 mL of heptane were added to each tube. Following mixing and centrifugation (4400 rpm, 5 min), the heptane layer containing fatty acid methyl esters (FAME) was analyzed using a gas chromatograph (GC) (7890A GC systems, Agilent Technologies Inc., Santa Clara, CA, USA) equipped with a flame ionization detector. FAME were separated on an Agilent HP-INNOWAX capillary column (30 m × 0.25 mm × 0.25 μm). Oven temperature was kept at 90 °C for 1 min, then heated to 235 °C at 10 °C/min, and held at 235 °C for 5 min. Hydrogen was used as a carrier gas. EPA and DHA were identified by comparing retention times with those of authentic standards. Fish oil loading efficiency was calculated according to Eq. (1):

$$LE (\%) = \frac{\text{Experimental loading capacity}}{\text{Theoretical loading capacity}} \times 100 \quad (1)$$

where, experimental loading capacity is the total mass of EPA + DHA in the solid lipid particles, and theoretical loading capacity is the total mass of EPA + DHA in the physical blends of fish oil and FHSO, of which initial fish oil concentration was 30%.

2.4. Particle size and size distribution analysis

A particle size analyzer (Mastersizer 3000, Malvern Instruments Ltd., Worcestershire, UK) was used to measure the particle size and size distribution of the 30% fish oil-loaded solid lipid particles before and after each stage of *in-vitro* digestion. Prior to digestion, samples (30 mg) were dispersed in 25 mL distilled water containing polyoxyethylene sorbitan monooleate (Tween 80) as an emulsifier (0.4%, w/w). After vortexing for 10 seconds, the suspensions were sonicated for 30 min in an ultrasonic water bath (3510 R-MTH, Branson Ultrasonics Corporation, Danbury, CT, USA) before analysis. Oral, gastric, and intestinal samples were analyzed without the addition of Tween 80 and sonication. Intestinal sample was diluted using distilled water (pH 7.0) (1:10, v/v)

to avoid multiple scattering effect.²¹ The refractive index (RI) was set as 1.46 with distilled water (RI= 1.33) as dispersant. Each measurement started when the obscuration value reached 5-7%. The average particle sizes are reported as the volume-weighted mean diameter (d_{43}).

2.5. Scanning Electron Microscope (SEM) analysis

A field emission scanning electron microscope (FE-SEM) (S4700, Hitachi High-Technologies Corporation, Japan) was used to analyze the morphology of the 30% fish oil-loaded solid lipid particles. A thin layer of sample was spread onto a double-sided carbon tape attached onto a sample mount, and sputter coated with chromium in argon atmosphere using a HiPace 80 (Pfeiffer Vacuum, Germany).

2.6. Confocal Fluorescence Microscope analysis

A confocal fluorescence microscope (A1R-Ti2 confocal system, Nikon Instruments Inc., Tokyo, Japan) coupled with a 60× oil immersion objective lens was used to monitor the microstructures of the fish oil-loaded solid lipid particles after each stage of *in-vitro* digestion. Approximately 5 mg of solid samples (prior to digestion, top phase after oral and gastric digestion) or 40 μ L of liquid samples (bottom phase after oral and gastric digestion, and intestinal samples) were firstly stained with 40 μ L of Nile Red solution (100× dilution of 1.25% stock solution, w/v, in propane-1,2-diol) for 40 min before image collection. Excitation wavelength of 561.6 nm and emission wavelength of 570 – 620 nm were set to conduct the analysis for red fluorophores. An aliquot of sample was placed on a microscope slide, covered by a cover slip, and then microstructure images were acquired using image analysis software (NIS-Elements, Nikon, Melville, NY). The imaging was carried out at room temperature (21 °C).

2.7. Simulated digestion

A sequential oral, gastric, and intestinal digestion was performed according to the method of Minerkus *et al.*³⁹ and Ubeyitogullari *et al.*⁴⁰ with slight modifications. The final Ca^{2+} concentration was kept at 10 mM.⁴¹ Simulated digestion fluids, i.e., simulated salivary fluid (SSF, pH 7.0), simulated gastric fluid (SGF, pH 3.0), and simulated intestinal fluid (SIF, pH 7.0) were prepared according to Minerkus *et al.*³⁹ and Ubeyitogullari *et al.*⁴⁰ However, NaHCO_3 was replaced by NaCl at the same molar ratio⁴² for all the simulated digestion fluids in this study, as suggested by Mat *et al.*⁴² All enzyme units were calculated based on the enzyme activity declared by the manufacturers. An automatic titration (pH-stat) unit (835 Titrand, Metrohm USA, Inc., Riverview, FL) was used to monitor the pH throughout the whole sequential digestion experiment. Crude fish oil, bulk FHSO, hollow solid lipid particles, and the physical mixture of crude fish oil and empty particles/bulk FHSO were used as controls. Total lipid amount of the samples subject to *in-vitro* digestion was kept the same.²¹

2.7.1. Simulated oral digestion

Simulated oral digestion was conducted according to Ubeyitogullari *et al.*⁴⁰ with a few modifications. Briefly, 14 mL of SSF electrolyte stock solution was added into the vessel circulated with 37 °C water of the pH-stat unit. Then, the sample (0.32 g) and α -amylase solution (2 mL, 750 U mL⁻¹) were added into the vessel to obtain a final α -amylase concentration of 75 U mL⁻¹. Next, 3.948 mL of distilled water and 50 μL of 5 M CaCl_2 were included. Then, the pH of the mixture was adjusted to 7.0. Finally, the mixture was incubated at 37 °C with a continuous agitation at 150 rpm for 30 s.

2.7.2. Simulated gastric digestion

Following the oral digestion, 13 mL of SGF electrolyte stock solution was added into the vessel and the pH of the mixture was adjusted to 3.0 using 0.108 mL of 1 M HCl solution. Then, porcine pepsin (2 mL, 40000 U mL⁻¹) and fungal lipase (1 mL, 1000 U mL⁻¹) solutions were included. Afterwards, 10 µL of 5 M CaCl₂ and 3.882 mL of distilled water were added. Therefore, the final ratio of oral bolus to SGF solution was achieved at 50:50 (v/v). Finally, the mixture was incubated at 37 °C with a continuous agitation at 100 rpm for 2 hours. The pH was monitored and kept at 3.0 throughout the gastric digestion using the pH-stat unit.

2.7.3. Simulated intestinal digestion

Gastric chyme sample (40 mL) was mixed with 24.5 mL of SIF electrolyte stock solution. Then, 5 mL of pancreatin solution with amylase activity of 3200 U mL⁻¹ was added to achieve a final α-amylase activity of 200 U mL⁻¹. Extra porcine pancreatic lipase (3310 U) was included into the pancreatin solution to have a final lipase activity of 2000 U mL⁻¹ in the final mixture.^{39,40} Next, 2.5 mL of 0.32 M fresh bile solution, 7.3 mL of distilled water and 100 µL of 5 M CaCl₂ were added into the vessel. The pH was subsequently adjusted to 7.0 using 0.4 mL of 1 M NaOH solution. Therefore, the final ratio of gastric chyme to SIF solution was obtained at 50:50 (v/v). Finally, the mixture was incubated at 37 °C with a continuous agitation at 100 rpm for 2 hours. The pH was monitored throughout the intestinal digestion and maintained at pH 7.0 by titrating appropriate volume of 1 M NaOH solution using the pH-stat unit. The volume of the 1 M NaOH added to the vessel was recorded, and the amount of free fatty acids (FFA) released at the small intestine phase was calculated using the following Eq. (2)²¹:

$$FFA (\%) = \frac{V_{NaOH} \times m_{NaOH} \times m_{lipid}}{w_{lipid} \times 2} \times 100 \quad (2)$$

where, V_{NaOH} is the volume of titrant consumed in liters, m_{NaOH} is the molarity of the NaOH solution used (1 M), m_{lipid} is the molecular weight of the sample, w_{lipid} is the weight of sample in the digestion system in grams (0.32 g).

2.8. Obtaining the bioaccessible fraction after the simulated digestion

Digestate samples at the end of the sequential simulated digestion were placed in an ice bath to stop digestion and centrifuged at $10,000\times g$ and $4\text{ }^{\circ}\text{C}$ for 35 min and filtered⁴³ to separate any undigested oil from the aqueous phase (bioaccessible fraction) and pellet. The bioaccessible fraction was then collected with the fine tip of a disposable pipette, quantified using a graduated cylinder and stored at $-80\text{ }^{\circ}\text{C}$ until oil extraction.

2.9. Oil extraction from the bioaccessible fraction

The oil presented in the aqueous phase after simulated digestion was extracted by hexane (1:3; supernatant:hexane, v/v). The mixture was vortexed for 10 min. Then the mixture was centrifuged at $3000\times g$ for 2 min to separate the hexane fraction.^{44,45} The extraction procedure was repeated three times. The hexane fraction was evaporated off using a rotary evaporator (BÜCHI Rotavapor R-200, New Castle, DE, USA) equipped with a heating bath (BÜCHI Heating Bath B-490, New Castle, DE, USA) at $30\text{ }^{\circ}\text{C}$ to obtain the digested oil. Residual solvent was further removed by flushing it with nitrogen. The oil extracts were kept at $-80\text{ }^{\circ}\text{C}$ until GC analysis (as described in Section 2.3). The bioaccessibility of the EPA + DHA was calculated using the following Eq. (3):

$$\text{Bioaccessibility (\%)} = \frac{\text{EPA + DHA in the bioaccessible fraction}}{\text{Total EPA + DHA included in the sample}} \times 100 \quad (3)$$

2.10. Statistical analysis

Data are presented as mean \pm standard deviation based on triplicate experiments and analyses. A single factor ANOVA was used to analyze differences among the samples in fatty acid composition (%), mean particle diameter (μm), free fatty acid released (%) and EPA + DHA bioaccessibility (%). SAS version 9.3 was the statistical software package used for all analyses (SAS Institute Inc., NC, USA). An alpha level of <0.05 was used to denote significance. Post hoc test was conducted using Tukey's multiple comparison.

3. Results and discussion

3.1. Characterization of the fish oil-loaded particles

SEM images of empty particles and fish oil-loaded particles are shown in Fig. 1. Both empty particle and the fish oil-loaded particles were spherical, intact and in the form of free-flowing powder. Empty particles had a smooth surface (Fig. 1 a-b), whereas the presence of fish oil resulted in formation of a wrinkled surface (Fig. 1 c-d). During mixing of CO_2 and lipids (FHSO + fish oil), CO_2 dissolved in the lipid mixture and the lipid mixture expanded at the bottom of the expansion vessel. When the SC- CO_2 -expanded lipid mixture is atomized at the nozzle upon depressurization, a liquid droplet of FHSO, fish oil, and CO_2 mixture was formed and then this droplet turned into a liquid lipid bubble due to expansion of the CO_2 at the atmospheric pressure.⁶ At the same time, temperature of the atomized particles suddenly decreased due to Joule-Thomson effect.²⁴ Upon cooling, the liquid FHSO bubble as the particle shell solidified and loaded with fish oil. No apparent cracks or breakages were observed on the particles, which is important to better protect fish oil from oxidation.⁶ The wrinkles presented on the surface of the fish oil-loaded particles was due to different solubilities of the CO_2 in the FHSO and fish oil and therefore led to different solidification rates from the liquid lipid bubble to solid lipid spheres during atomization. It was reported that CO_2 has a higher solubility in the lower melting point lipids than the higher

melting point counterparts which contributes to higher volumetric expansion.^{46,47} When fish oil was incorporated with FHSO, more CO₂ was dissolved in the lipid mixture and consequently the formed lipid droplet during atomization contained more CO₂. The presence of more CO₂ in the liquid lipid droplet resulted in more force exerted on the liquid lipid bubble. Then the liquid lipid bubble solidified at a lower cooling rate due to its lower melting point and there was more time to create irregular non-smooth surface during particle formation.⁶

Both empty particles and the fish oil-loaded particles presented a bimodal size distribution (Fig. 2). The mean particle size of the empty particles and the fish oil-loaded particles was 5.3 ± 0.9 and 6.9 ± 1.0 μm , respectively, and 10% of the total volume of the solid lipid particles were at nano size (Fig. 2). The presence of the nanoparticles was confirmed by the TEM analysis in our previous report.⁶ The slightly larger particle size of the fish oil-loaded particles was due to higher concentration of CO₂ in the lipid mixture and therefore yielded particles with a higher CO₂ expansion during atomization compared to empty particles.

The fatty acid profile was analyzed to examine the effect of particle formation on EPA and DHA retention. Table 1 shows the composition of the major fatty acids in the fish oil, FHSO, physical blend of fish oil and FHSO, and the fish oil-loaded solid lipid particles. There was no significant difference in total polyunsaturated fatty acids (PUFA) before and after particle formation ($p>0.05$) except a slight drop occurred in DHA from 1.8 to 1.6% ($p<0.05$), indicating that the particle formation process did not negatively cause fish oil degradation. Fish oil loading efficiency was achieved at $92.3\pm 1.6\%$.

3.2. Effect of *in-vitro* digestion on the particle size, size distribution and morphology

Figs. 3 and 4 illustrate the volume-weighted mean particle diameter and particle size distribution of the fish oil-loaded particles as they passed through the simulated *in-vitro* digestion

stages, respectively. Initially, the mean particle diameter (d_{43}) was $6.9\pm 1.0\ \mu\text{m}$ and exhibited bimodal size distribution. The hollow structure of the fish oil-loaded particles was confirmed with confocal microscopy images where the black cavity presented (Fig. 5a). After passing through the oral phase, the mean particle diameter increased to $15.2\pm 1.5\ \mu\text{m}$ while the pattern remained bimodal. The confocal microscopy images (Fig. 5b) showed that the particles slightly aggregated on the top phase under simulated oral conditions as compared to the initial stage (Fig. 5a). On one hand, the presence of the aqueous fluids increased the repulsion between the lipid particles and the aqueous phase; therefore, lipid particles gathered together. On the other hand, a previous study suggested that droplet aggregation may be caused by bridging or depletion flocculation induced by mucin in the simulated saliva.²⁵ Bridging flocculation occurs due to the mucin binding to two or more oil droplets' surface, whereas depletion flocculation occurs due to elevated osmotic attractive forces between the droplets caused by non-adsorbed mucin.²⁵ The bottom phase of the oral digesta was also analyzed by confocal microscope (Fig. 5c). It was found that a small portion of the sample freely passed into the aqueous fluids possibly due to the small particle size (nanoparticles).

After passing through the gastric phase, the fish oil-loaded particles exhibited an increase in mean particle diameter to $32.4\pm 2.0\ \mu\text{m}$ (Fig. 3) and showed an additional size distribution greater than $100\ \mu\text{m}$ (Fig. 4). Moreover, it is worth noting that agglomeration of the particles on the top phase became more pronounced as detected by confocal microscopy (Fig. 5d), which could be an explanation for the increase in the particle size. The observed increase in particle aggregation (Fig. 5d) can be attributed to a few phenomena. Firstly, relatively high ionic strength of the simulated gastric fluids repulsed lipid particles and in turn have reduced the strength of the electrostatic repulsion between the lipid particles.²¹ Secondly, the anionic mucin molecules from simulated

saliva may have facilitated bridging flocculation of the lipid particles in acidic gastric phase.²⁵ Thirdly, the gastric lipase presented in this digestion stage may have partially hydrolyzed the outer FHSO shell, which could have altered the positioning of the lipid particles. Similar to the oral bottom phase, a small portion of the sample (Fig. 5e) was identified in the gastric bottom phase, which was related to the nanoparticles transferred into the aqueous fluids and partially digested fish oil-loaded particles or surface fish oil.

After exposure to the small intestinal phase, the mean particle diameter remained relatively high ($d_{43} = 24.0 \pm 1.7 \mu\text{m}$) and there were still large aggregates (Fig. 4). However, the size of these aggregates was significantly lower than those after the gastric phase ($p < 0.05$) (Fig. 3; Fig. 5f). The composition and structure of the digesta in the small intestinal fluids after lipid digestion is highly complex.⁴⁸ Therefore, it is difficult to identify the constituents and particles presented in the digesta (Fig. 5f), since they may include digested broken particle pieces, undigested fish oil-loaded particles, free fatty acids, monoacylglycerols, bile salts, and enzymes. These constituents can assemble into several types of colloidal substances with various morphologies, dimensions and aggregation states, including micelles, vesicles, and insoluble calcium salts.²¹ Therefore, *in-vitro* digestibility and EPA + DHA bioaccessibility need to be assessed to better understand the lipid digestion of the fish oil-loaded particles and to complement particle size and confocal microscopy measurements.

3.3. *In-vitro* digestibility

The *in-vitro* digestibility of the fish oil-loaded hollow solid lipid particles was examined by measuring the released FFA after exposure to SGF-SIF. As expected, no pH change was observed during the simulated oral and gastric digestion for all samples (data not shown), which was attributed to the low extent of lipid digestion by salivary and gastric enzymes. On the other

hand, FFA produced during simulated gastric digestion did not alter the pH of the lipolysis media since they were non-ionized at this pH.⁴⁹ Figure 6 presents the rate of FFA released (lipolysis) during the 2-hour simulated intestinal digestion. All samples exhibited a gradual lipid digestion process. The bulk FHSO had $18.4\pm 3.1\%$ lipolysis while the empty particles made of FHSO achieved $45.1\pm 0.8\%$ ($p < 0.05$). The highest lipolysis was observed for fish oil-loaded hollow solid lipid particles ($68.4\pm 1.3\%$), followed by physical mixtures of empty particles and fish oil ($56.3\pm 0.6\%$) and physical mixtures of bulk FHSO and fish oil ($44.0\pm 0.7\%$) ($p < 0.05$). In both cases, the particle formation process converting bulk FHSO to empty particles and the loading fish oil into the hollow solid lipid particles significantly facilitated lipolysis throughout the small intestinal digestion. Small particle size and high surface area improved lipolysis by increasing the exposure of lipids to lipases, yielding FFA and/or monoacylglycerols, and by increasing the adsorption of bile salts onto the lipids. Bile salts play an important role in regulating lipid digestion; they replace phospholipids at the oil-water interface to facilitate lipase binding, restore lipase activity and also solubilize FFA to reduce the interfacial accumulation.⁵⁰ These results suggest that the encapsulation of fish oil in the hollow solid lipid particles improved overall lipid digestibility. In a similar study, Augustin *et al.*⁴¹ examined *in-vitro* digestion of microencapsulated oil powders stabilized with different proteins or mixtures of protein and carbohydrates. The lipolysis of the canola oil in these products varied between 12-68%, while in comparison, neat canola oil only had 1.08% lipolysis.⁴¹ In our study, the lipolysis of crude fish oil was $98.4\pm 2.6\%$. However, it should be noted that the lipolysis of crude fish oil was not comparable to the other tested samples, since the rest of the samples included FHSO at varying contents. Therefore, both FHSO and fish oil contributed to lipolysis in those samples rather than only fish oil itself. In agreement with our findings, Lin *et al.*³⁶ reported that emulsification improved lipolysis, with 50 wt% algal oil

emulsion (23.5%) significantly higher than the physical mixture of algal oil, soy lecithin and water (7.3%) at initial stage in duodenal digestion ($p < 0.05$).

3.4. EPA and DHA bioaccessibility

Measuring bioaccessibility after *in-vitro* digestion is important because it provides information to assess health benefits of the loaded bioactive compounds and to adequately give nutritional significance to health claims.⁵¹ A sufficient delivery of omega-3 PUFAs to the intestine could be beneficial to reduce the incidence of some diseases due to its anti-inflammatory properties.⁴³ Bioaccessibility refers to the amount of available digested lipids (FFA and monoacylglycerols) that can be absorbed by intestinal epithelium cells. It is widely acknowledged that micellar solubilization of long-chain PUFAs such as EPA and DHA can be less efficient than short- and medium-chain fatty acids, since long chains lead to lower solubility and adversely affects their partitioning between oil and aqueous.^{36,52} Figure 7 shows the bioaccessibility of EPA + DHA available in the aqueous phase after sequential simulated digestion. Fish oil-loaded particles had the highest proportion of EPA + DHA ($18.2 \pm 1.3\%$) transferred to the aqueous phase ($p < 0.05$), followed by the physical mixture of empty particles and fish oil ($14.0 \pm 0.4\%$) and crude fish oil ($9.7 \pm 0.4\%$), with physical mixture of bulk FHSO and fish oil being the lowest ($5.0 \pm 0.3\%$). Even though crude fish oil achieved a nearly complete lipolysis, subsequent measurements of lipid solubilization by bile salts showed the EPA + DHA transfer from oil to the aqueous phase was low. This suggests a lack of interaction between the free fatty acids and/or monoacylglycerols and bile salts, therefore leading to a low formation of mixed micelles to transport to the aqueous phase. The higher EPA + DHA bioaccessibility from the fish oil-loaded particles was associated with the larger oil-water interface presented at the beginning of the small intestinal digestion, allowing lipases and bile salts to attach to the long-chain PUFAs with higher surface area, which offers

better emulsification. In addition, it could also be due to less surfactant needed to form mixed micelles with the fish oil-loaded particles than the crude fish oil, thereby facilitating FFA solubilization. Previously, Lin *et al.*³⁶ concluded that the emulsification of DHA-rich algal oil facilitated digestive lipolysis and subsequent DHA bioaccessibility. In another study, Joyce *et al.*⁴⁹ microencapsulated fish oil within porous silica particles and the microencapsulated fish oil was 1.4-fold more bioaccessible than the commercial fish oil.

4. Conclusions

Fish oil-loaded hollow solid lipid micro- and nanoparticles were generated by atomization of the CO₂-expanded lipid mixture. The obtained particles were spherical and free-flowing with an average particle size of 6.9 µm. Fish oil loading efficiency was achieved at 92.3% (w/w). This study examined the digestive stability, digestibility, and EPA + DHA bioaccessibility of the micro- and nano-encapsulated fish oil using an *in-vitro* sequential digestion approach. The mean particle diameter increased markedly after oral (15.2 µm) and gastric (32.4 µm) digestion and then decreased after the small intestinal stage (24.0 µm). Fish oil-loaded particles remained spherical and intact but mainly agglomerated on the top phase throughout the oral and gastric digestion. However, a mixed digesta was formed after the small intestinal digestion. The extent of lipolysis was significantly increased for the 30% fish oil-loaded particles as compared to the physical mixtures of empty particles or bulk FHSO with fish oil ($p < 0.05$), which was attributed to the small particle size with large surface area. Moreover, EPA and DHA bioaccessibility was significantly improved from 9.7 to 18.2% with the 30% fish oil-loaded particles ($p < 0.05$). The results from this study should provide valuable information about the potential applications of fish oil delivery through foods and beverages in the form of hollow solid lipid micro- and nanoparticles.

Conflict of interest

Authors declare no conflicts of interest.

Acknowledgements

We gratefully acknowledge the financial support by the United States Department of Agriculture, National Institute of Food and Agriculture (USDA NIFA) (Accession Number 1011129). The research was performed in part in the Nebraska Nanoscale Facility: National Nanotechnology Coordinated Infrastructure and the Nebraska Center for Materials and Nanoscience (and/or NERCF), which are supported by the National Science Foundation under Award ECCS: 1542182, and the Nebraska Research Initiative. Special thanks to Dr. You Zhou and Dirk Anderson from the center for their assistance in confocal fluorescence microscopy analysis.

References

- 1 B. Michelsen, S. L. Madsen and P. Gotfredsen, in *Guide to Functional Food Ingredients*, ed. J. Young, Leatherhead Publishing, Surrey, England, 2001, Polyunsaturated fatty acids, pp. 141-195.
- 2 S. C. Larsson, M. Kumlin, M. Ingelman-Sundberg and A. Wolk, Dietary long-chain n-3 fatty acids for the prevention of cancer: A review of potential mechanisms, *Am. J. Clin. Nutr.*, 2004, **79**, 935-945.
- 3 K. Lane, E. Derbyshire, W. Li and C. Brennan, Bioavailability and potential uses of vegetarian sources of omega-3 fatty acids: a review of the literature, *Crit. Rev. Food Sci. Nutr.*, 2014, **54**, 572-579.
- 4 E. Arab-Tehrany, M. Jacquot, C. Gaiani, M. Imran, S. Desobry and M Linder, Beneficial effects and oxidative stability of omega-3 long-chain polyunsaturated fatty acids, *Trends Food Sci. Technol*, 2012, **25**, 24-33.

- 5 W. E. M. Lands, *Fish omega-3 and human health* (2nd ed.), AOCS Press, Champaign, Illinois, USA, 2005.
- 6 J. Yang and O. N. Ciftci, Encapsulation of fish oil into hollow solid lipid micro- and nanoparticles using carbon dioxide, *Food Chem.*, 2017, **231**, 105-113.
- 7 M. Aghbashlo, H. Mobli, A. Madadlou and S. Rafiee, The correlation of wall material composition with flow characteristics and encapsulation behavior of fish oil emulsion, *Food Res. Int.*, 2012, **49**, 379-388.
- 8 M. Aghbashlo, H. Mobli, A. Madadlou and S. Rafiee, Influence of wall material and inlet drying air temperature on the microencapsulation of fish oil by spray drying, *Food Bioprocess Tech.*, 2013, **6**, 1561-1569.
- 9 Z. Shen, C. Apriani, R. Weerakkody, L. Sanguansri and M. A. Augustin, Food matrix effects on *in vitro* digestion of microencapsulated tuna oil powder, *J. Agric. Food Chem.*, 2011, **59**, 8442-8449.
- 10 L. Sanguansri and M. A. Augustin, in *Functional food ingredients and nutraceuticals: Processing technologies*, ed. J. Shi, CRC Press/Taylor and Francis Group, Boca Raton, 2006, Microencapsulation and delivery of omega-3 fatty acids, pp. 297-327.
- 11 C. J. Barrow, C. Nolan and Y. Jin, Stabilization of highly unsaturated fatty acids and delivery into foods, *Lipid Technol.*, 2007, **19**, 108-111.
- 12 M. A. Augustin, L. Sanguansri and O. Bode, Maillard reaction products as encapsulants for fish oil powders, *J. Food Sci.*, 2006, **71**, E25-E32.
- 13 W. Kolanowski, D. Jaworska, J. Brodt and B. Kunz, Sensory assessment of microencapsulated fish oil powder, *J. Am. Oil Chem.' Soc.*, 2007, **84**, 37-45.

- 14 M. Choi, U. Ruktanonchai, S. Min, J. Chun and A. Soottitantawat, Physical characteristics of fish oil encapsulated by β -cyclodextrin using an aggregation method or polycaprolactone using an emulsion-diffusion method, *Food Chem.*, 2010, **119**, 1694-1703.
- 15 Y. H. Cho, H. K. Shim and J. Park, Encapsulation of fish oil by an enzymatic gelation process using transglutaminase cross-linked proteins, *J. Food Sci.*, 2003, **68**, 2717-2723.
- 16 Z. Zhang, E. A. Decker and D. J. McClements, Encapsulation, protection, and release of polyunsaturated lipids using biopolymer-based hydrogel particles, *Food Res. Int.*, 2014, **64**, 520-526.
- 17 R. Wang, Z. Tian and L. Chen, A novel process for microencapsulation of fish oil with barley protein, *Food Res. Int.*, 2011, **44**, 2735-2741.
- 18 C. Chung, L. Sanguansri and M. A. Augustin, *In vitro* lipolysis of fish oil microcapsules containing protein and resistant starch, *Food Chem.*, 2011, **124**, 1480-1489.
- 19 K. Moomand and L. Lim, Properties of encapsulated fish oil in electrospun fibres under simulated *in vitro* conditions, *Food Bioprocess Tech.*, 2015, **8**, 431-444.
- 20 S. L. Kosaraju, R. Weerakkody and M. A. Augustin, *In-vitro* evaluation of hydrocolloid-based encapsulated fish oil, *Food Hydrocoll.*, 2009, **23**, 1413-1419.
- 21 C. E. Gumus, E. A. Decker and D. J. McClements, Gastrointestinal fate of emulsion-based ω -3 oil delivery systems stabilized by plant proteins: Lentil, pea, and faba bean proteins, *J. Food Eng.*, 2017, **207**, 90-98.
- 22 Y. Tan, K. Xu, L. Li, C. Liu, C. Song and P. Wang, Fabrication of size-controlled starch-based nanospheres by nanoprecipitation, *ACS Appl. Mater. Interfaces*, 2009, **1**, 956-959.
- 23 S. M. Jafari, E. Assadpoor, Y. He and B. Bhandari, Encapsulation efficiency of food flavours and oils during spray drying, *Dry Technol.*, 2008, **26**, 816-835.

- 24 J. Yang and O. N. Ciftci, Formation of hollow solid lipid micro- and nanoparticles using supercritical carbon dioxide, *Food Bioprod Process*, 2016, **98**, 151-160.
- 25 R. Zhang, Z. Zhang, H. Zhang, E. A. Decker and D. J. McClements, Influence of lipid type on gastrointestinal fate of oil-in-water emulsions: *In vitro* digestion study, *Food Res. Int.*, 2015, **75**, 71-78.
- 26 S. Marze, A. Meynier and M. Anton, *In vitro* digestion of fish oils rich in *n*-3 polyunsaturated fatty acids studied in emulsion and at the oil-water interface, *Food Funct.*, 2013, **4**, 231-239.
- 27 M. C. Michalski, C. Genot, C. Gayet, C. Lopez, F. Fine, F. Joffre, et al., Multiscale structures of lipids in foods as parameters affecting fatty acid bioavailability and lipid metabolism, *Prog. Lipid Res.*, 2013, **52**, 354-373.
- 28 P. Reis, K. Holmberg, H. Watzke, M. E. Leser and R. Miller, Lipases at interfaces: A review, *Adv. Colloid Interface Sci.*, 2009, **147-148**, 237-250.
- 29 D. J. McClements, E. A. Decker and Y. Park, Controlling lipid bioavailability through physicochemical and structural approaches, *Crit. Rev. Food Sci. Nutr.*, 2009, **49**, 48-67.
- 30 P. J. Wilde and B. S. Chu, Interfacial & colloidal aspects of lipid digestion, *Adv. Colloid Interface Sci.*, 2011, **165**, 14-22.
- 31 D. J. McClements, E. A. Decker, Y. Park and J. Weiss, Designing food structure to control stability, digestion, release and absorption of lipophilic food components, *Food Biophys.*, 2008, **3**, 219-228.
- 32 S. Mun, E. A. Decker and D. J. McClements, Influence of emulsifier type on *in vitro* digestibility of lipid droplets by pancreatic lipase, *Food Res. Int.*, 2007, **40**, 770-781.
- 33 C. Chung, L. Sanguansri, and M. A. Augustin, Effects of modification of encapsulant materials on the susceptibility of fish oil microcapsules to lipolysis, *Food Biophys.*, 2008, **3**, 140-145.

- 34 U. Klinkesorn and D. J. McClements, Influence of chitosan on stability and lipase digestibility of lecithin-stabilised tuna oil-in-water emulsions., *Food Chem.*, 2009, **114**, 1308-1315.
- 35 I. Ikeda, E. Sasaki, H. Yasunami, S. Nomiyama, M. Nakayama, M. Sugano, et al., Digestion and lymphatic transport of eicosapentaenoic and docosahexaenoic acids given in the form of triacylglycerol, free acid and ethyl ester in rats, *Biochim. Biophys. Acta*, 1995, **1259**, 297-304.
- 36 X. Lin, Q. Wang, W. Li and A. J. Wright, Emulsification of algal oil with soy lecithin improved DHA bioaccessibility but did not change overall *in vitro* digestibility, *Food Funct.*, 2014, **5**, 2913-2921.
- 37 D. Eratte, K. Dowling, C. J. Barrow and B. P. Adhikari, *In-vitro* digestion of probiotic bacteria and omega-3 oil co-microencapsulated in whey protein isolate-gum Arabic complex coacervates, *Food Chem.*, 2007, **227**, 129-136.
- 38 H. D. Belayneh, R. L. Wehling, E. Cahoon and O. N. Ciftci, Extraction of omega-3-rich oil from *Camelina sativa* seed using supercritical carbon dioxide, *J. Supercrit. Fluids*, 2015, **104**, 153-159.
- 39 M. Minekus, M. Alming, P. Alvito, S. Ballance, T. Bohn, C. Bourlieu, et al., A standardised static *in vitro* digestion method suitable for food - an international consensus, *Food Funct.*, 2014, **5**, 1113-1124.
- 40 A. Ubeyitogullari, R. Moreau, D. Rose, J. Zhang and O. N. Ciftci, Enhancing the bioaccessibility of phytosterols using nanoporous corn and wheat starch bioaerogels. *Eur. J. Lipid Sci. Tech.*, 2019, **121**, 1700229.
- 41 M. A. Augustin, L. Sanguansri, J. K. Rusli, Z. Shen, L. J. Cheng, J. Keogh, et al., Digestion of microencapsulated oil powders: *in vitro* lipolysis and *in vivo* absorption from a food matrix, *Food Funct.*, 2014, **5**, 2905-2912.

- 42 D. J. L. Mat, S. L. Feunteun, C. Michon and I. Souchon, *In vitro* digestion of foods using pH-stat and the INFOGEST protocol: Impact of matrix structure on digestion kinetics of macronutrients, proteins and lipids, *Food Res. Int.*, 2016, **88**, 226-233.
- 43 H. Ilyasoglu and S. N. El, Nanoencapsulation of EPA/DHA with sodium caseinate-gum arabic complex and its usage in the enrichment of fruit juice, *LWT - Food Sci. Technol.*, 2014, **56**, 461-468.
- 44 P. Calvo, M. Lozano, A. Espinosa-Mansilla and D. González-Gómez, *In-vitro* evaluation of the availability of ω -3 and ω -6 fatty acids and tocopherols from microencapsulated walnut oil, *Food Res. Int.*, 2012, **48**, 316-321.
- 45 A. M. Cheong, C. P. Tan and K. L. Nyam, *In-vitro* gastrointestinal digestion of kenaf seed oil-in-water nanoemulsions, *Ind. Crops Prod.*, 2016, **87**, 1-8.
- 46 O. N. Ciftci and F. Temelli, Melting point depression of solid lipids in pressurized carbon dioxide, *J. Supercrit. Fluids*, 2014, **92**, 208-214.
- 47 E. Jenab and F. Temelli, Density and volumetric expansion of carbon dioxide-expanded canola oil and its blend with fully-hydrogenated canola oil, *J. Supercrit. Fluids*, 2012, **70**, 57-65.
- 48 M. F. Yao, H. Xiao and D. J. McClements, Delivery of lipophilic bioactives: assembly, disassembly, and reassembly of lipid nanoparticles, *Annu. Rev. Food Sci. Technol.*, 2014, **5**, 53-81.
- 49 P. Joyce, H. Gustafsson and C. A. Prestidge, Enhancing the lipase-mediated bioaccessibility of omega-3 fatty acids by microencapsulation of fish oil droplets within porous silica particles, *J. Funct. Foods*, 2018, **47**, 491-502.

- 50 D. J. McClements and Y. Li, Structured emulsion-based delivery systems: Controlling the digestion and release of lipophilic food components, *Adv. Colloid Interface Sci.*, 2010, **159**, 213-228.
- 51 P. Ercan and S. N. El, Changes in content of coenzyme Q10 in beef muscle, beef liver and beef heart with cooking and *in vitro* digestion, *J. Food Compos. Anal.*, 2011, **24**, 1136-1140.
- 52 L. Sek, C. J. H. Porter, A. M. Kaukonen and W. N. Charman, Evaluation of the *in-vitro* digestion profiles of long and medium chain glycerides and the phase behavior of their lipolytic products, *J. Pharm. Pharmacol.*, 2002, **54**, 29-41.

Table 1. Major fatty acid composition (%) of fish oil, FHSO, their physical blend^a, and the obtained fish oil-loaded hollow solid lipid particles^b.

Composition	Fish oil (FO)	FHSO	FO-Mix	FO-P
Myristic acid (14:0)	9.7±0.2	-	2.3±0.0 a	2.1±0.0 b
Palmitic acid (16:0)	20.7±0.3	11.7±0.1	13.9±0.2 a	13.6±0.2 a
Palmitoleic acid (16:1)	14.4±0.2	-	3.3±0.0 a	2.8±0.0 b
Stearic acid (18:0)	4.0±0.1	88.3±1.4	69.9±1.1 a	69.8±0.6 a
Oleic acid (18:1)	8.7±0.1	-	2.1±0.0 a	2.0±0.0 b
Linoleic acid (18:2)	1.8±0.0	-	0.4±0.0 a	0.3±0.0 b
Linolenic acid (18:3)	1.4±0.0	-	0.3±0.0 a	0.3±0.0 a
Octadecatetraenoic acid (18:4)	3.1±0.0	-	0.5±0.1 a	0.5±0.0 b
Arachidonic acid (20:4)	1.8±0.0	-	0.3±0.0 a	0.3±0.0 a
EPA (20:5)	15.5±0.3	-	3.4±0.2 a	3.2±0.1 a
DHA (22:6)	10.5±0.2	-	1.8±0.0 a	1.6±0.1 b
SFA	34.4±0.6	100.0±1.5	86.1±1.3 a	85.5±0.8 a
MUFA	23.1±0.3	-	5.4±0.0 a	4.8±0.0 b
PUFA	34.1±0.5	-	6.7±0.3 a	6.2±0.2 a

^a FO-Mix: physical mixture of 30% fish oil and 70% FHSO.

^b FO-P: Fish oil-loaded hollow solid lipid particles.

EPA: eicosapentaenoic acid; DHA: docosahexaenoic acid; SFA: saturated fatty acids; MUFA: monounsaturated fatty acids; PUFA: polyunsaturated fatty acids.

Different letters within the same row represent significant differences (p<0.05).

Figure captions

Fig. 1. Scanning electron microscope (SEM) images of the (a, b) empty hollow solid lipid particles, and (c, d) fish oil-loaded hollow solid lipid particles.

Fig. 2. Particle size distribution of the empty hollow solid lipid particles and fish oil-loaded hollow solid lipid particles.

Fig. 3. Volume-weighted mean particle diameter of the fish oil-loaded hollow solid lipid particles after exposure to different stages of the simulated *in-vitro* digestion. Different letters represent significant differences among the mean particle diameter ($p < 0.05$).

Fig. 4. Particle size distribution of the fish oil-loaded hollow solid lipid particles after exposure to different stages of the simulated *in-vitro* digestion.

Fig. 5. Microstructures of the fish oil-loaded hollow solid lipid particles after exposure to different stages of the simulated *in-vitro* digestion. a) initial; b) after oral stage – top phase; c) after oral stage – bottom phase; d) after gastric stage – top phase; e) after gastric stage – bottom phase; and f) after small intestinal stage. Red fluorescence color indicates presence of fish oil in the particles. Black cavity of the particles indicates hollow structure.

Fig. 6. Release of free fatty acids from lipid samples during simulated small intestinal digestion.

Fig. 7. EPA + DHA bioaccessibility (%) in the bioaccessible fraction after simulated digestion. Different letters represent significant differences among the bioaccessibility values of EPA + DHA ($p < 0.05$).

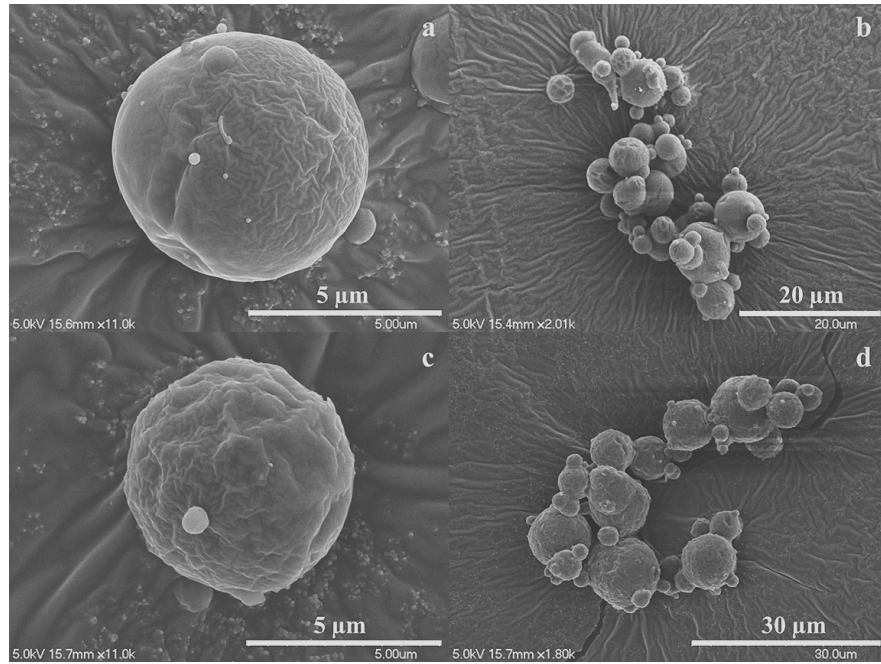


Figure 1

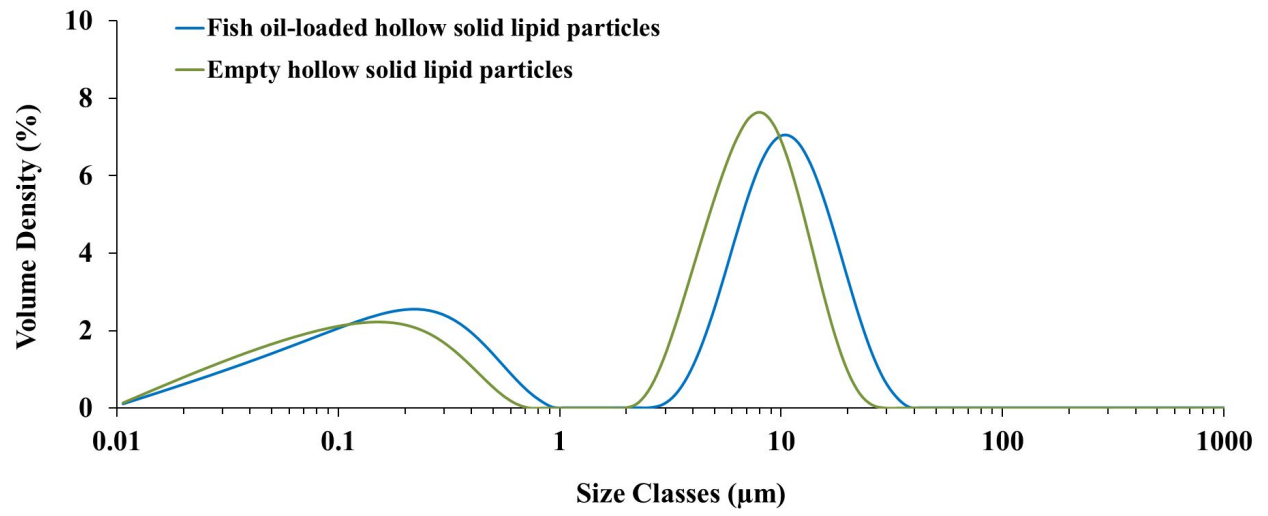


Figure 2

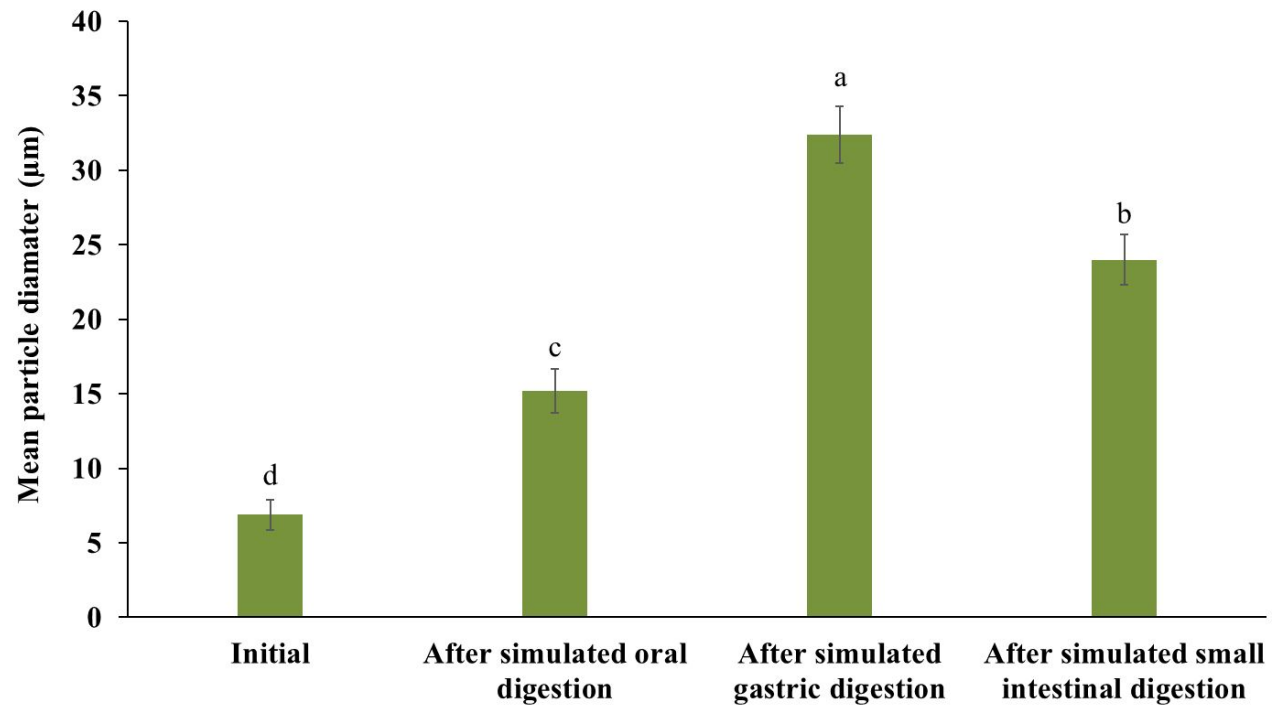


Figure 3

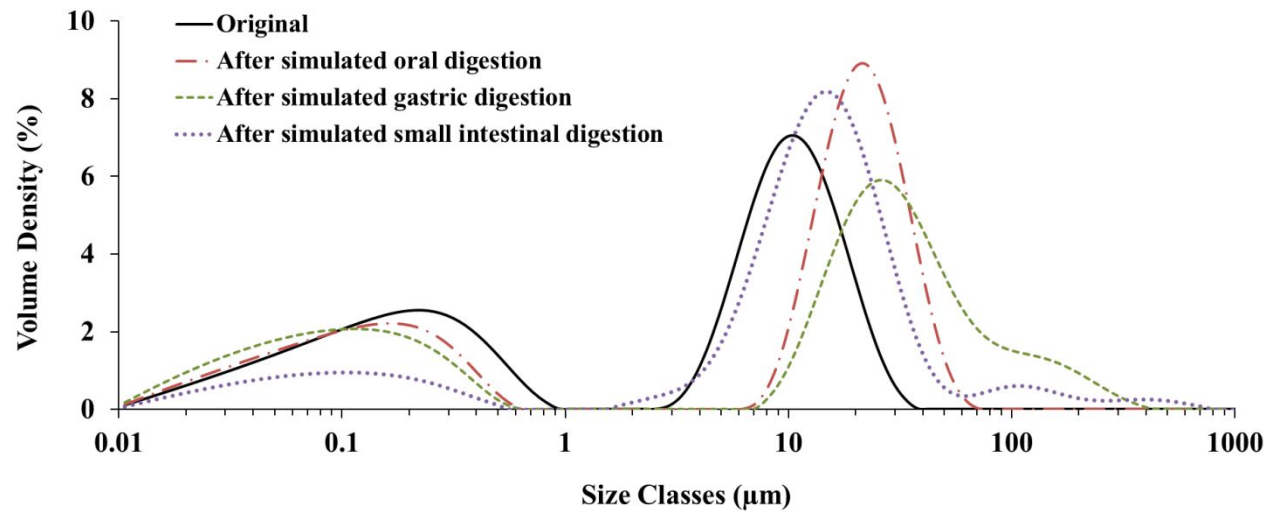


Figure 4

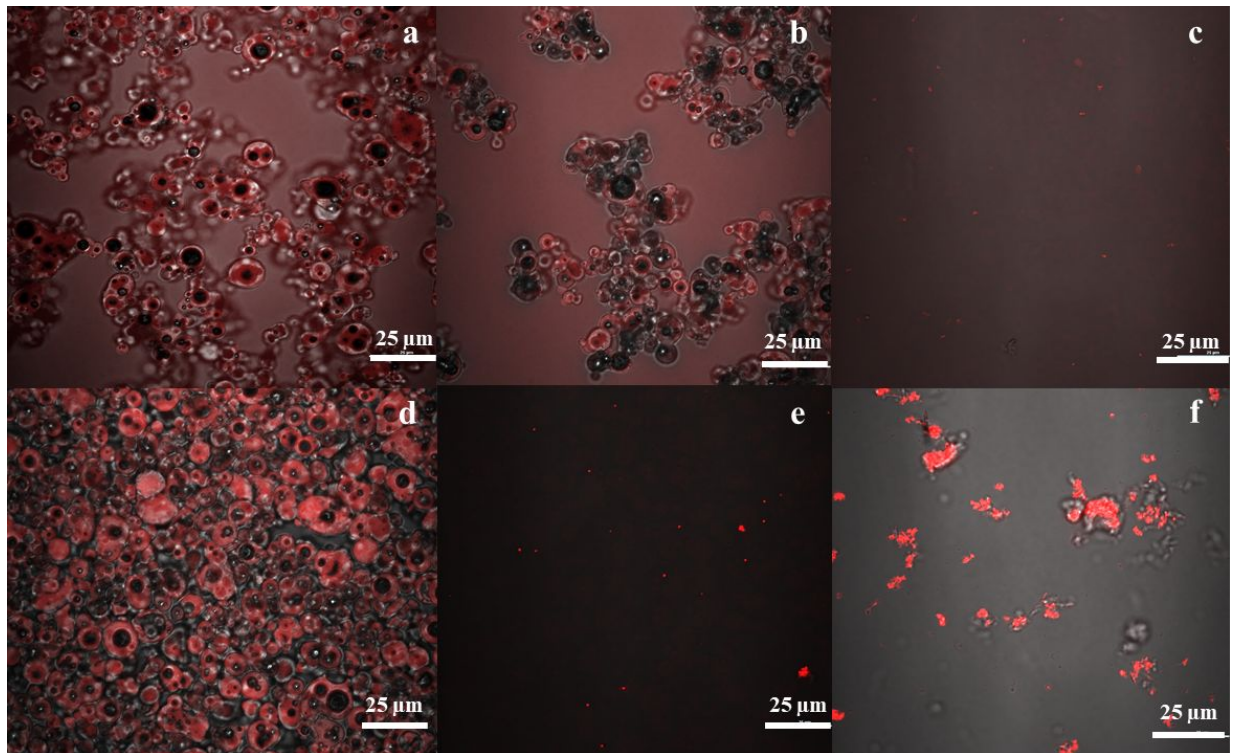


Figure 5

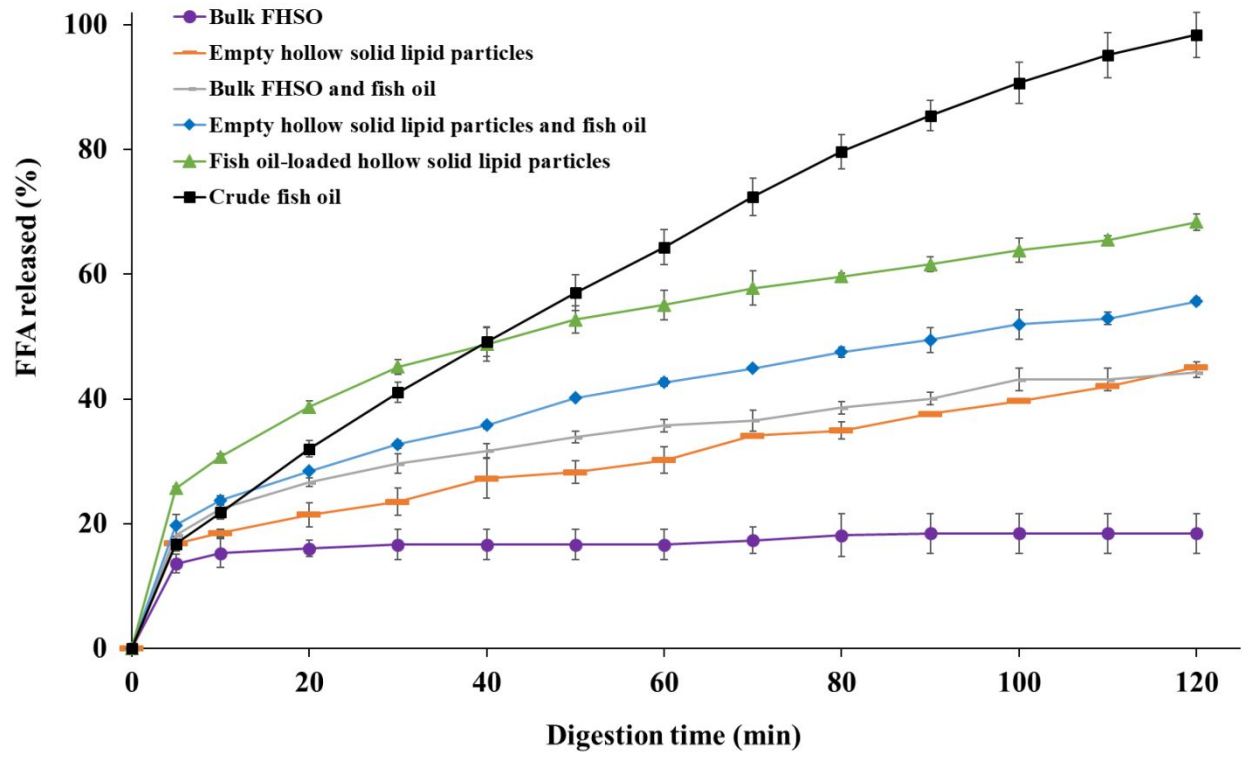


Figure 6

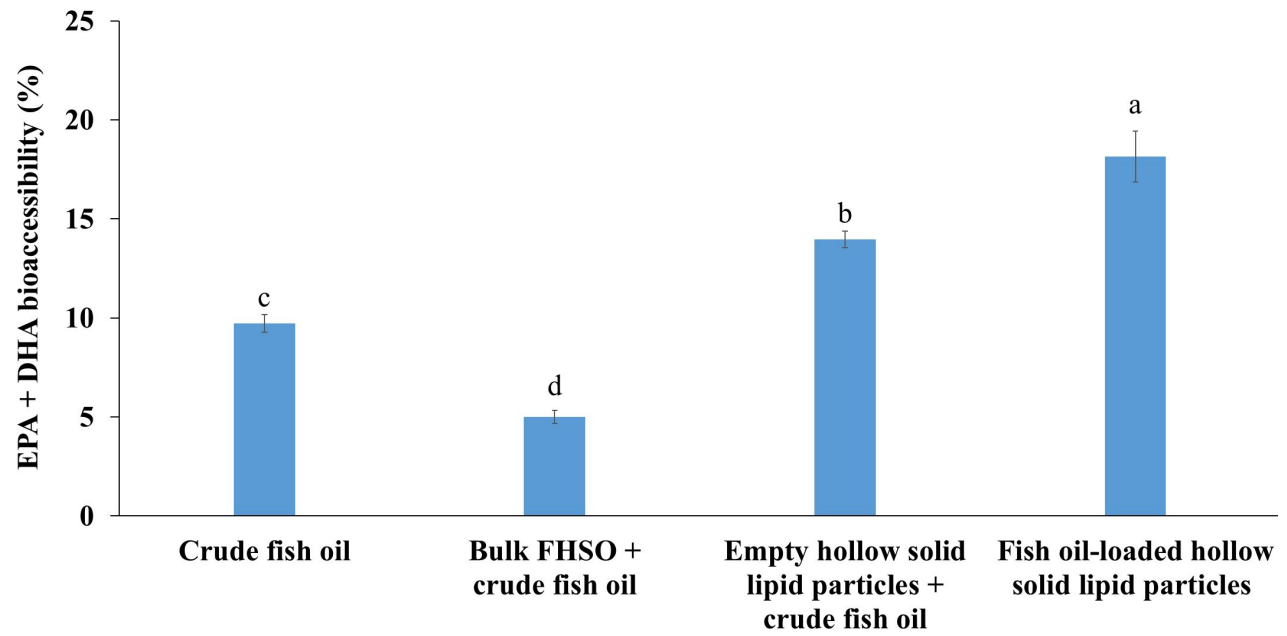
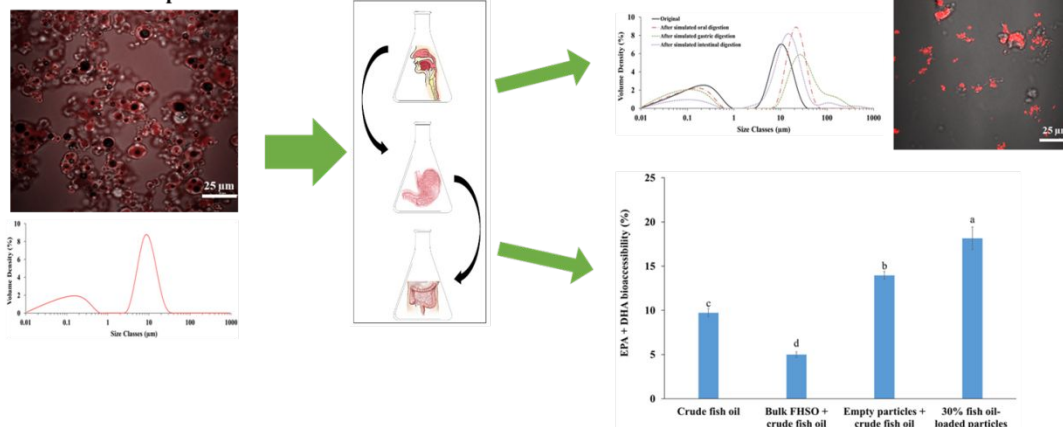


Figure 7

Graphical Abstract

Fish oil-loaded hollow solid lipid micro- and nanoparticles



This study reports *in vitro* bioaccessibility of first-of-their-kind fish oil-loaded hollow solid lipid micro and -nanoparticles formed using a green method based on supercritical fluid technology. Eicosapentaenoic acid (EPA) and docosahexaenoic acid (DHA) bioaccessibility was improved from 9.7 to 18.2% when fish oil was loaded into hollow solid lipid particles.